Bi-objective Optimization of Axial Profile of Pin Fin with Uniform Base Heat Flux

Tao Dong [d,*,†] Zhongyuan Shi [a,b,c,†] Atle Jensen [c]

a. Institute of Applied Micro-Nano Science and Technology, Chongqing Key Laboratory of Colleges and Universities on Micro-Nano Systems Technology and Smart Transduction, National Research Base of Intelligent Manufacturing Service
Chongqing Technology and Business University, 19 Xuefu Ave., Nan'an District, Chongqing, China;

b. Chongqing Engineering Laboratory for Detection, Control and Integrated System
Chongqing Technology and Business University, 19 Xuefu Ave., Nan'an District, Chongqing, China;

c. Department of Mathematics
Faculty of Mathematics and Natural Sciences, University of Oslo, P.O box 1053, Blindern, 0316 Oslo, Norway;

d. Department of Microsystems
Faculty of Technology, Natural Sciences and Maritime Sciences, University College of Southeast Norway (HSN), Raveien 215, 3184 Borre, Norway.

* The corresponding authors' email address: Tao.Dong@usn.no; zhongyuan.shi@ctbu.edu.cn

† The authors - Tao Dong and Zhongyuan Shi share the first authorship.

Abstract

Cone shaped pin fin with curved profile and uniform base heat flux was investigated. The result from simultaneous optimization in regard of fin efficiency and total volume is presented. The profile is represented by the Non-Uniform Rational B-Spline (NURBS) for an additional degree of freedom to morph during the optimization process. An overall dominance was obtained from the present work, as compared to the classic concave parabolic profile, the practical constraint in fabrication taken into consideration. The profiles corresponding to the acquired Pareto solution sets tend to comply with the constructal law of design, in which freestream of heat flow is expected.

Keywords

pin fin; curved axial profile; NURBS; bi-objective optimization; constructal design

Nomenclature

T	Temperature, K
Bi_L	Biot Number
f	Curve Function of the Axial Pin Fin Profile, m
F	Dimensionless Curve Function of the Axial Pin Fin Profile
f_r	Reference Profile, see Eq. (4), m
h	Heat Transfer Coefficient, W/(m^2·K)
i	Indice for Control Points
k	Thermal Conductivity, W/(m·K), see Eq. (2) and Eq. (7); Indice for Breaking Points in a Knot Vector, see Eq. (10), Eq. (11) and Eq. (12); Order of the Basis Function for NURBS, see Eq. (10), Eq. (11) and Eq. (12)
L	Axial Length of Pin Fin, m
$\boldsymbol{n}$	Unit Normal Vector on the Axial Fin Profile Curve, Pointing outward to the Surrounding Fluid
N	Basis Function for NURBS
n	Total Number of Control Points
$\boldsymbol{p}$	Coordinate Vector of Control Points
q	Input Heat Flux from the Fin Base, W/m^2
r	Radial Coordinate, m
$\boldsymbol{r}$	Coordinate Vector of a Specific Point on NURBS
$\tilde{r}$	Dimensionless Radial Coordinate
$\tilde{r}_b$	Dimensionless Base Radius of Pin Fin

$\boldsymbol{T}$ Knot Vector

t Dependent Variable for the Basis Function of NURBS

T_0 Temperature of the Surrounding Fluid, K

V Dimensionless Fin Volume

w Weight Factor for NURBS

z Vertical Coordinate, Starting from the Fin Tip, m

$\tilde{z}$ Dimensionless Vertical Coordinate, Starting from the Fin Tip

Greek Symbols

α Half Tip Angle of Axial Fin Profile

η Fin Efficiency

θ Dimensionless Temperature

σ Deviation

Subscripts

T Temperature, see Eq. (15)

0 Surrounding Fluid

a Average (Eq. (16)) or Integral Average (Eq. (17))

b Base

1. Introduction

Aero- and space-based electronic applications that demands high-flux heat dissipation entails stringent requirement on weight and space occupation in the meanwhile [1][2]. Passive augmentation of cooling performance, which has been made available owing to the considerable development of micro fabrication, is thus particularly important with limited access to coolant fluid.

Pin fin structure, as one of the surface-extension-based techniques for heat transfer enhancement, has so far drawn attention from numerous investigators. Following the pioneering work on one-dimensional (1D) conductive-convective fins [3]-[7], Kundu and Das illustrated a unified method under Murray-Gardner assumptions for all three types of convectional fins, i.e. straight/longitudinal fin, annular fin and pin fin, by using the calculus of variation. Common features concerning temperature distribution, fin efficiency and optimum fin profile was discussed. Hajabdollahi et al. [8] carried out a bi-objective optimization, respectively on the two competing indices, the total heat transfer rate and the fin efficiency of 1D pin fin. The axial profile was approximated using a Bézier curve. The resultant Pareto frontier was elaborated with respect to the relevant the volume and heat transfer surface of the pin fin. Employing the same set of ODEs, along with the objective functions, Wang et al. [9] proposed a new algorithm that stepwise constructs and optimize the longitudinal fin by layers of truncated cone slabs. The optimum fin profile yields higher heat transfer rate from the base, of which the temperature was held constant, but lower fin efficiency and higher space occupation as compared to the result from Hajabdollahi [8]. Azarkish et al [10] reported the optimum profile of straight fin obtained from the genetic algorithm modified for monotonic variation in the x- and y-coordinates of the control points that constitute the B-spline which represents the fin profile. The longitudinal fin was modelled in a 1D energy equation, subject to constant base temperature, natural convection, radiation heat loss and volumetric heat generation uniformly distributed in the solid domain. The method was validated by comparing to the benchmark parabolic profile from literature [11][12]. The effect from variable and constant heat transfer coefficients was discussed. It was found that the impact of radiation on the optimum profile cannot be neglected, while increasing the base temperature and the volumetric heat generation is detrimental to fin efficiency. The authors [13] further exploited the optimization of fin array layout by modelling the net radiation heat flux in the two-dimensional (2D) unit that incorporates the two adjacent fins. Both the number of fins and the fraction of radiation in total heat transfer rate were reported in non-monotonic variation with the base temperature. The optimum fin profile does not affect the number of fins as compared to the cases with conventional fin profiles, albeit the heat transfer is slightly enhanced.

In comparison with the conventional 1D study, 2D analysis has raised concerns as well. Yeh [14] demonstrated the criteria of different Biot numbers in the optimization of aspect ratio and heat transfer rate of both longitudinal rectangular fin and cylindrical pin fin, with the consideration on fin tip convection. The error caused by conventional 1D analysis was illustrated with the proposed modification, as compared to the 2D solution. Fabbri [15] compared the 2D straight fin of rectangular and polynomial profile, with their tip and lateral surface exposed to different convection coefficient, and base temperature held constant. A considerable increase in the fin effectiveness was observed after implementing the genetic algorithm in the optimization in regard to polynomial coefficients. Also in a typical case, the fin with a fourth-order polynomial profile yields twice the heat flux as much as that dissipated from the rectangular one. The author [16] later presented the effect of undulated fin profile on the inner-tube-wall heat transfer enhancement, within the laminar regime. The impact from the inter-fin space and the thermal conductivity ratio between solid and fluid was discussed. The fin profile of higher-order polynomial does not necessarily bring higher flow resistance. The optimum profile was found more likely to be dominated by convection, rather than its own conductive characteristics. In terms of heat flux dissipation per unit tube length, asymmetric fins performs slightly better than symmetric ones with the same order of polynomial profile, although increasing the order for asymmetric fins does not result in very different performance [17]. Despite that very different patterns of enhancement were observed for asymmetric fins as compared to the preceding in-tube scenarios [18], Copiello and Fabbri [19] still furthered their exploration on the polynomial-based symmetric profile optimization of straight fin array with tip clearance, cooled by laminar convection in parallel channels. In the bi-objective genetic optimization aimed at minimizing the Nusselt number and the normalized flow resistance simultaneously, the heat transfer improvement by adopting the wavy fin profile stalled when the required flow resistance is lower than a certain threshold, whereas addition constraint on the fin volume may compromise the heat transfer enhancement. Bobaru and Rachakonda [20] employed the mesh-free Galerkin method in obtaining the optimum space of the fin array, as well as the optimum profile of each fin aligned periodically, with constant temperature on the back side of the common base plate and natural convection flow passing through in between. The optimum layout depends on the conductivity of the fin material, relative to external convection coefficient. High conductivity comes with fins with sharp tip and narrow base, while low conductivity tends to blunt fins with wide base. The investigation on the rectangular annular fin mounted on the outer wall of circular tube was presented by Kang and Look [21]. The tip and side walls of the fin are subject to different convection boundaries while the radiation is considered. The impact from geometric dimensions are elaborated in together the effect from the abovementioned thermal boundaries, note that the difference between 1D and 2D analyses is magnified as the fin top convection or the fin height increases. The analysis was later applied to the trapezoidal annular fin [22]. Iqbal et al. [23] applied the discontinuous Galerkin finite element method to the conjugate heat transfer optimization for the fins circumferentially mounted on the outer wall of the inner pipe in a pipe-in-pipe design. Represented by piecewise Hermite cubic splines, the optimum fin profile with bulk tip, where heat transfer coefficient is higher, and minuscule extrusion array all along the side wall, was strongly influenced by the number of fins and the geometric parameters of the annulus configuration. Considerable heat transfer enhancement was identified when compared to the trapezoidal, triangular and parabolic fins with equivalent pipe diameter. Based on the volume averaged momentum and energy equations, respectively with regard to velocity and temperature, Kim [24] believes that the optimized concave fins periodically distributed on the inner wall of a circular tube can bring up to 12% reduction in thermal resistance, referring to the case with straight fins. The correlation for the degree of improvement indicates the dependence on pumping power and tube length. Nguyen and Yang [25] proposed a modified Newton-Raphson method for the volume minimization of 2D straight fin, with a specified temperature and input heat flow rate at the fin base. The linear temperature distribution along the fin length was presented as a validation of the proposed method, when the concave parabolic profile from Schmidt [3] was applied. Lower volumes and higher fin efficiency are obtained for the cases with variable heat transfer coefficient along the profile boundary, in comparison with those from Azarkish et al. [10].

On the other hand, the constructal law, which was first proposed by Bejan as "For a finite-size system to persist in time (to live), it must evolve in such a way that it provides easier access to the imposed currents that flow through it." [26], marked the starting point of new era in regard to thermohydraulic designs, and has recently found applications in numerous areas including but not limited to pore network arrangement [27], solar energy utilization [28], phase change based heat storage [29] and so forth. The constructal law is also embodied as a common trend in the evolution of either animate or inanimate systems [30][31]. As far as fin shape optimization is concerned, Bejan provided a novel perspective that focuses on the effect of boundary shape on heat flow organization [32], taking the paradigm design from Schmidt as an example [3][33][34].

The literature review is indicating that the design optimization of curved pin fin with uniform input heat flux from the base bottom remains far less concerned. In the present study, the Pareto solution, which corresponds to the maximization of fin efficiency while holding the minimal fin volume, was obtained and compared to the classic concave parabolic profile. The fabrication and/or structural constraint on tip angle and the optimum-design-correlated constructal law are involved in the discussion, which may serve as the guideline for practical designs.

2. Problem Statement

2.1 Governing Equation and Boundary Conditions

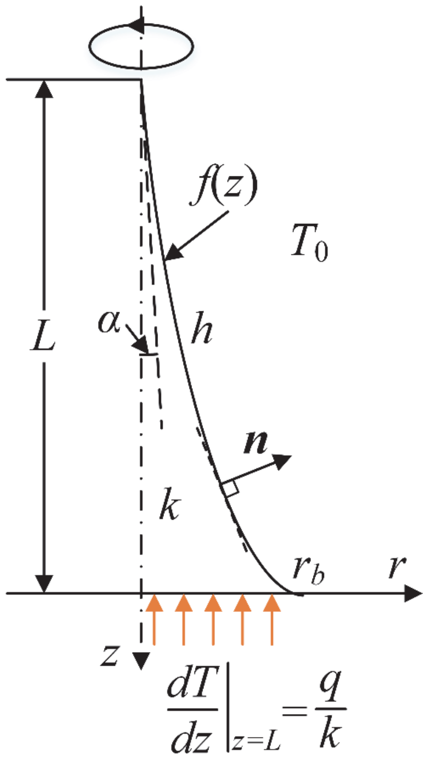

Fig. 1 Schematic Representation of the Curved Cone Fin for Heat Transfer Enhancement

Starting from the parabolic fin profile with “un-strangled” heat lines [35]-[37], the present work is aimed at the profile optimization of cone-shaped pin fin (see Fig. 1). Note that the original fin design is an extruded body with constant-cross-section composed of two parabolas enclosed by a straight line at the bottom, we are expecting a different profile of optimization, regarding the energy equation in the polar coordinate system as follows.

$$\frac{\partial^2 T}{\partial r^2}+\frac{\partial T}{r\partial r}+\frac{\partial^2 T}{\partial z^2}=0 \tag{1}$$

subject to

$$\begin{cases} z = L, \dfrac{\partial T}{\partial z} = \dfrac{q}{k} \\ r = 0, \dfrac{\partial T}{\partial r} = 0 \\ r = f(z), \dfrac{\partial T}{\partial \boldsymbol{n}} = \dfrac{h(T_0 - T)}{k} \end{cases} \tag{2}$$

where $\boldsymbol{n}$ is the normal vector pointing to the ambient fluid and can be represented in the r-z plane as

$$\boldsymbol{n} = \left(-\frac{f'(z)}{\sqrt{f'^2(z) + z^2}}, \frac{z}{\sqrt{f'^2(z) + z^2}} \right) \tag{3}$$

for any given point (z, $f(z)$) on the fin boundary, while

$$f_r(z) = r_b \left(\frac{z}{L}\right)^2 \tag{4}$$

is an reference/control group for the optimization. Resembling the scenario in which the heat “flows” only longitudinally (parallel to the z axis) [1], the optimized $f(z)$ is expected to be in such a way that the norm of radial temperature gradient is minimized throughout the entire solid domain. After normalization, Eqs. (1)-(3) become

$$\frac{\partial^2 \theta}{\partial \tilde{r}^2} + \frac{\partial \theta}{\tilde{r} \partial \tilde{r}} + \frac{\partial^2 \theta}{\partial \tilde{z}^2} = 0, \tag{5}$$

the boundary condition being

$$\begin{cases} \tilde{z} = 1, \dfrac{\partial \theta}{\partial \tilde{z}} = 1 \\ \tilde{r} = 0, \dfrac{d\theta}{d\tilde{r}} = 0 \\ \tilde{r} = F(\tilde{z}), \dfrac{d\theta}{d\boldsymbol{n}} = -Bi_L\theta \end{cases} \tag{6}$$

where

$$\begin{cases} \tilde{z}, \tilde{r} = \dfrac{z, r}{L} \\ \theta = \dfrac{k(T - T_0)}{qL} \\ Bi_L = \dfrac{hL}{k} \\ F(\tilde{z}) = \dfrac{f(z)}{L}, \text{and accordingly } F'(\tilde{z}) = f'(z) \end{cases} \tag{7}$$

2.2 Axial Fin Profile Representation

The Non-Uniform Rational B-Spline (NURBS) [38] has been widely utilized in modern CAD/CAM/CAE due to its generality and excellent properties in geometry representation. The definition of a NURBS curve begins with the basis function

$$N_{i,k}(t) = \begin{cases} 1, t_i \le t < t_{i+1}, k = 1 \\ 0, t < t_i \ or \ t \ge t_{i+1}, k = 1 \\ \dfrac{t - t_i}{t_{i+k-1} - t_i} N_{i,k-1}(t) + \dfrac{t_{i+k} - t}{t_{i+k} - t_{i+1}} N_{i+1,k-1}(t), k > 1 \end{cases} \tag{8}$$

where t_i, as the ith breaking point (knot), constitutes the non-descending knot vector

$$\boldsymbol{T} = [t_0, t_1, \ldots, t_{n+k}]. \tag{9}$$

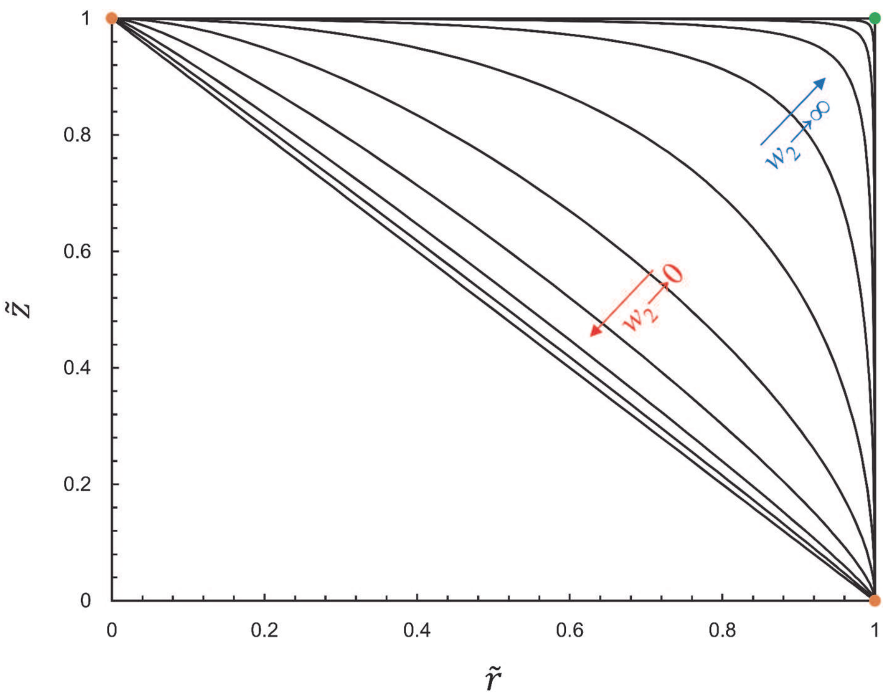

Fig. 2. The effect of weight factor in NURBS. Two orange control points are anchored at (0,1) and (1,0) respectively, the rest green one rendered freedom to morph as its corresponding weight factor w_2 changes.

As a linear combination of the above–defined basis functions, the NURBS curve is given by

$$\boldsymbol{r}(t) = \frac{\sum_{i=0}^{n} w_i \boldsymbol{p_i} N_{i,k}(t)}{\sum_{i=0}^{n} w_i N_{i,k}(t)}, n \geq k-1, t_{k-1} \leq t \leq t_{n+1}, w_i > 0 \tag{10}$$

in which $\boldsymbol{p_i}$ is the ith control point and w_i is the weight factor for $\boldsymbol{p_i}$. In the present study, the knot vector comes with the first k knots equal to each other. The same rule applies to the last k knots so that the two ending points of the resultant NURBS curve was anchored to the first and the last control points, in regard of the rest n-k+1 internal knots. As an exemplary case shown in Fig. 2, the variation of w_2 for the second one (marked in green) leads to a series of different curves that lies within the convex hull formed by connecting the adjacent control points (0,0), (1,1) and (1,0), which hold invariant. Adding the weight factor in general render more degrees of freedom for the NURBS curve to morph than any of its specific case in which, for instance, all the weight factors are equal to 1 [8][10][13][25].

As an anchored control point, the fin tip in the present work is at (0,1) in the $\tilde{r}$-$\tilde{z}$ coordinate system. The other anchored control point represents the end of the profile curve that meets the base plane of the pin fin, which is free to move along the $\tilde{r}$ axis. All the rest control points are free to move in the $\tilde{r}$-$\tilde{z}$ plane, with the following constraint to avoid the generation of unphysical curves [10].

$$\begin{cases} \tilde{r}_{p_{i-1}} \le \tilde{r}_{p_i} \le \tilde{r}_{p_{i+1}} \\ \tilde{r}_{p_0} = 0, \tilde{r}_{p_n} = \tilde{r}_b \\ \tilde{z}_{p_{i+1}} \le \tilde{z}_{p_i} \le \tilde{z}_{p_{i-1}} \\ \tilde{z}_{p_0} = 1, \tilde{z}_{p_n} = 0 \end{cases}, 1 \le i \le n-1 \tag{11}$$

2.3 Bi-objective Optimization

The bi-objective optimization is to find the $F(\tilde{z})$ that corresponds to the Pareto frontier constituted by the fin efficiency

$$\eta = \frac{\tilde{r}_b^2}{2Bi_L \int_0^1 F(\tilde{z})\sqrt{1+F'^2(\tilde{z})}\theta_b(\tilde{z})d\tilde{z}} \tag{12}$$

to be maximized and the fin volume

$$V = \int_0^1 \pi F^2(\tilde{z})d\tilde{z} \tag{13}$$

to be minimized, simultaneously. Note that the existence of Pareto frontier from the above-defined bi-objective problem is hypothesized by considering the following two scenarios. In the first scenario, the axial pin fin profile is shaped as the modified Dirac delta function (the function value being unity at zero, instead of infinity). The fin efficiency is in essence zero as no path is available for conduction heat flow in this case. Alternatively, the fin volume is maximized covering the semi-infinite space ($0 \leq \tilde{z} \leq 1$ and $\tilde{r} \geq 0$) for the second scenario, which is again a trivial profile since it is merely an extra layer of thermal resistance. An optimum set of profiles is expected with finite fin volumes and higher fin efficiencies, between the aforementioned two scenarios of extremity.

The constraint concerning the manufacturability and/or structural integrity of needle-tipped pin fin is

$$F'(\tilde{z}) \geq \tan\alpha\,, 0 \leq \tilde{z} \leq 1 \tag{14}$$

where α defines the half-tip-angle (HTA) as is also indicated in Fig. 1. The finite volume method [39] was adopted to acquire the temperature field. The definition of fin efficiency in Eq. (8) is based on the 1D "heat tube" analysis [32], i.e. assuming a unidirectional upward heat flow within any cylindrical shell of infinitesimal thickness, where $\tilde{r}$ holds invariant. Based on the definition of the normalized deviation

$$\sigma_T = \frac{1}{F(\tilde{z})}\int_0^{F(\tilde{z})} \left|\frac{\theta - \theta_a}{\theta_a}\right| d\tilde{r} \tag{15}$$

in which

$$\theta_a = \frac{1}{F(\tilde{z})} \int_0^{F(\tilde{z})} \theta \, d\tilde{r} \tag{16}$$

and the integrally averaged deviation

$$\sigma_{Ta} = \int_0^1 \sigma_T \, d\tilde{z}, \tag{17}$$

the validity of the assumption will be discussed in the next section. The Pareto solution was obtained by employing the Non-dominated Sorting Genetic Algorithm – II (NSGA-II) [40]. The open-source code is available at [41] from its original developer.

3. Result and Discussion

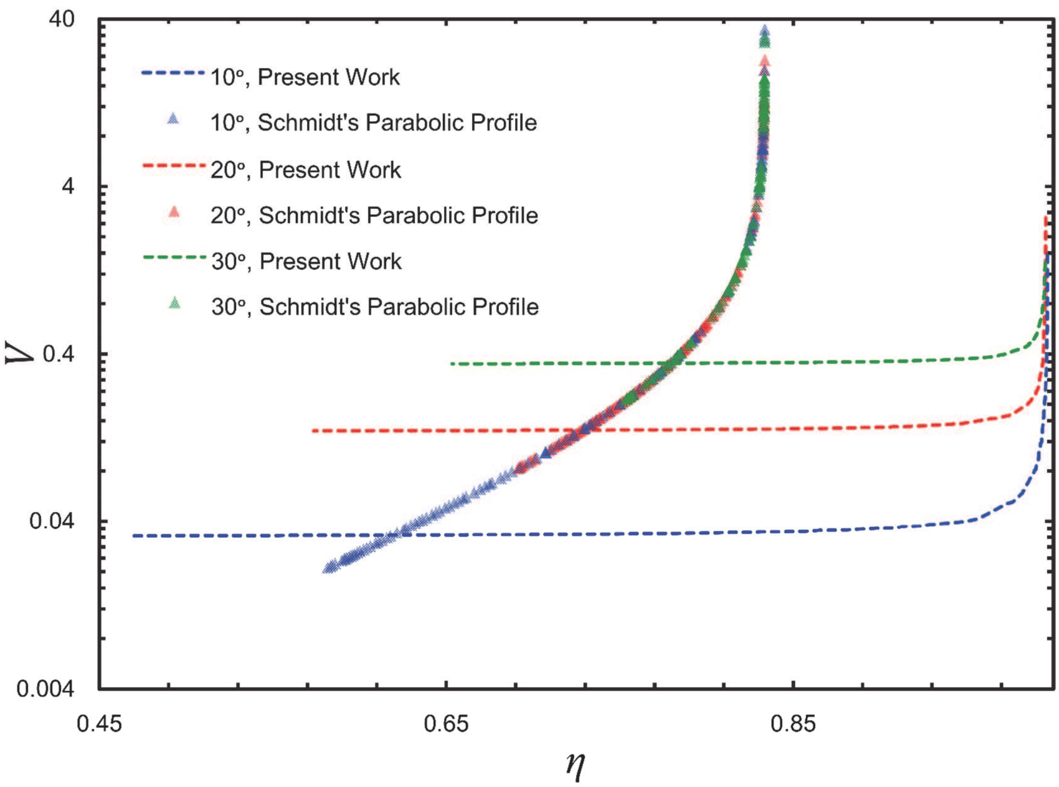

Fig. 3. The Pareto frontiers from present work versus that from the pin fin with classic concave parabolic profile, with different HTA constraints

The Pareto frontier obtained from Schmidt's parabolic profile was mostly dominated by that of the cases with all HTA constraints in the present work, for the same sets of pin fin height and base radius, as shown in Fig. 3. Nonetheless, the parabolic profile does take part of the dominance when the fin efficiency η is less than approximately 0.62, 0.77 and 0.78 respectively for the 10º, 20º and 30º HTA constraints, which stems from the fact that the region corresponds to the fin profile that is nearly identical to the baseline cone, while the pin fin with concave parabolic profile goes beyond the line that separate the feasible region (where the HTA constraint applies) from the infeasible in the present work. The fin efficiency was found much more sensitive, in contrast to the parabolic one, with the increment of fin volume as it starts to grow, the dominance later facilitated by a sharper turn into plateau where η no longer benefits from further increase of the fin volume.

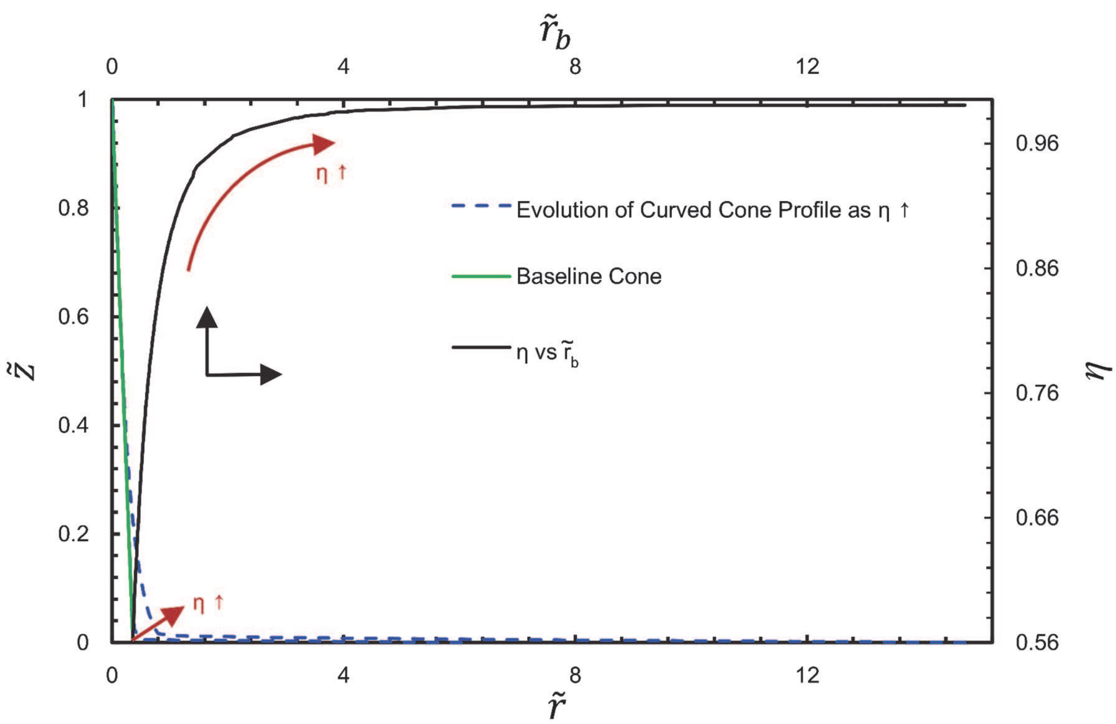

Fig. 4. Fin profiles from present work (with the 20º HTA constraint), along with the fin efficiency η versus the base radius r_b, in correspondence with the Pareto frontier.

Fig. 4 shows the general trend of the morphing profile, in regard to the Pareto frontier of 20º HTA constraint in Fig. 3 as the efficiency η increases. The increasing of η is synchronous to the process of sharp corner being rounded "additively", as the profile is getting away from the baseline cone. The evolution of fin efficiency is identifiable, when the increase in fin volume is accompanied by the expanding base radius. The simultaneous optimization with regard to the efficiency and volume of pin fin leads to a dimensionless base radius of over 14, which is unlikely the case in practice. However, the very nature of the Pareto optimization provides a mechanism of compromise. Complying with the law of diminishing marginal return, the normalized base radius being greater than 3.6 makes a difference of less than 4%, as the fin efficiency is concerned, for the constrained cases with 20º half tip angle. A similar trend from the cases with 10º and 30º HTA constraints was found.

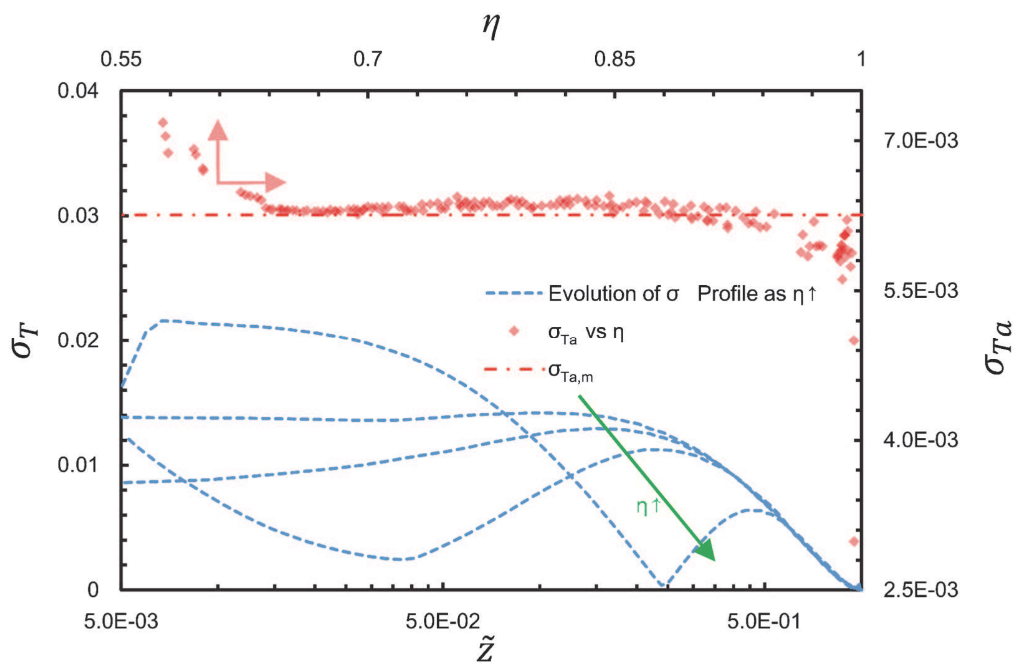

Fig. 5. The deviation profiles from present work (with the 20º HTA constraint), along with its integral mean versus the fin efficiency η, in correspondence with the Pareto frontier.

In Fig. 5, the first half of the normalized deviation (σ_T) profile is multimodal as the corresponding "slice" "marches" from the root to tip of the pin fin. For $\tilde{z} \geq 0.5$, the deviation profiles merge into a monotonous descending track. Together with the rapid decline in the beginning and ending section, and the plateau in the middle, the integrally averaged deviation (σ_{Ta}) in general decreases with increasing η, as is inferable from the representative profile of deviation (σ_T). The maximum σ_{Ta} not exceeding 0.73%, the mean of the σ_{Ta} profile is merely 0.63%. Such low value is expected for the previous 1D "heat tube" analysis [32] to hold, i.e. the temperature variation in the radial direction is in general negligible and the resultant "heat tube" would most likely indicate the free stream of heat flow. This seems applicable for the cases with both the 20º and 30º HTA constraints. Nonetheless, it is not necessarily valid if the σ_{Ta} profile with 10º HTA constraint is further introduced for comparison in Fig. 6. A descending-ascending profile becomes more prominent in the beginning when the base radius is less than 4, as compared with its counterpart with higher HTA constraint. Moreover, the cliff-jump was replaced by an abrupt uprising after the similar oscillating period, as $\tilde{r}_b$ approaches its high end. Starting with lower $\tilde{r}_b$, the case with lower HTA constraint comes with a steeper rise initially, before turning into the plateau. This is indicating sharper-tip pin fin that approximates the modified Dirac delta function benefits more from the "additively rounded corner".

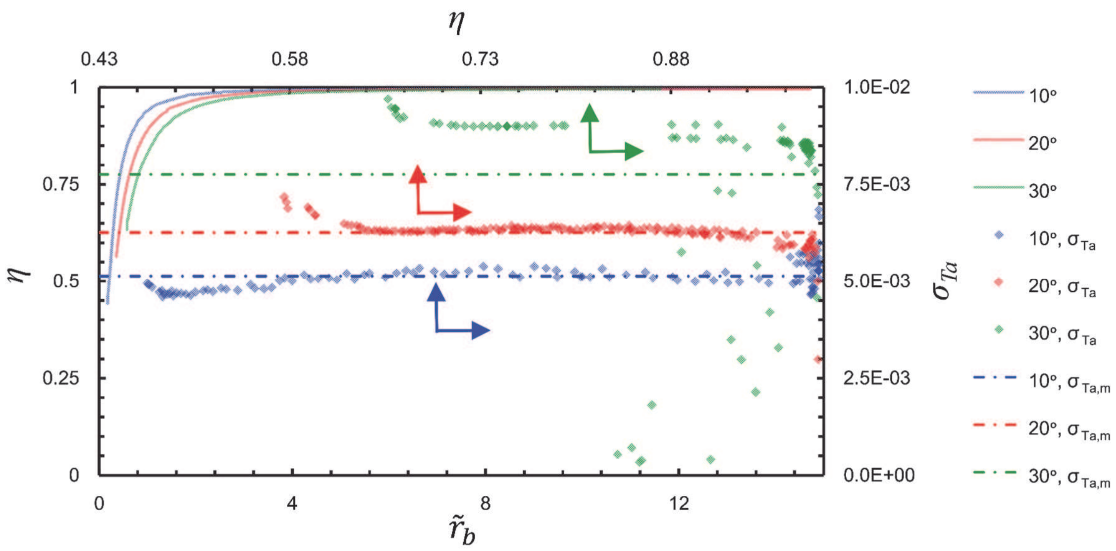

Fig. 6 Fin efficiency η versus fin base radius r_b, with different HTA constraints; the individual and mean of averaged temperature deviations for the cases on Pareto frontier.

4. Concluding Remarks

The present work focuses on the bi-objective optimization, which incorporates the impact of axial pin fin profile on its efficiency and volume. The practical concerns on fin tip angle are included in the investigation and the following conclusions are drawn:

- The pin fin with classic concave parabolic profile in general yield lower efficiency and higher space occupation as compared to the resultant profiles (with the same base radius) from the present work, except for those going beyond the afore-set HTA constraint.
- As the fin efficiency proceeds toward its upper limit, the corresponding fin profile evolves resembling the process in which the sharp-cornered void between the baseline cone and the fin base plane are being rounded. The process is accompanied by the diminishing return in terms of efficiency gain, as the fin base radius increases. Lower

HTA constraint is more sensitive to the abovementioned profile evolution in the initial stage.

- The temperature deviation calculated from the Pareto fin profiles essentially conforms to the requirement for the 1D analysis, and the constructal law which stipulates least-strangled heatlines throughout the entire computational domain. Note that lower deviation is not bound to higher fin efficiency for a certain HTA constraint.

Acknowledgment

The present work, partly derived from the author's (Zhongyuan Shi <zhongyus@uio.no> at University of Oslo) Ph.D. thesis, is supported by Trilobite Microsystems AS and Sensovann AS.

The research is funded in part by National Natural Science Foundation of China (No. 11702045 and 61650410655), Chongqing Research Program of Basic Research and Frontier Technology (No. cstc2015jcyjBX0004, cstc2015jcyjA20023, cstc2017jcyjA1842), EU Erasmus+ Capacity Building in Higher Education (No. 573828-EPP-1-2016-1-BG-EPPKA2-CBHE-JP), Innovation Team of Chongqing Universities and Colleges – Smart Micro-Nano Systems Technology and Application (No. CXTDX201601025) and Science and Technology Research Program of Chongqing Education Commission (No. KJ1600602 & No. KJ15006XX).

The financial support from Forskningsradet Nærings-Ph.D. (Project No.: 251129), Regionale Forskningsfond Oslofjordfondet (Project No.: 258902 and 260586) and NANO2021 (Project No.: 263783) is hereby acknowledged.

The authors are grateful for the comments from all reviewers.

Reference

[1] Tuckerman D B, Pease R F W. High-performance heat sinking for VLSI[J]. IEEE Electron Device Letters, 1981, 2(5): 126-129.

[2] İzci T, Koz M, Koşar A. The effect of micro pin-fin shape on thermal and hydraulic performance of micro pin-fin heat sinks[J]. Heat Transfer Engineering, 2015, 36(17): 1447-1457.

[3] Schmidt E. Die Wärmeübertragung durch Rippen[M]. 1926.

[4] Duffin R J. A variational problem relating to cooling fins[J]. J. Math. Mech, 1959, 8(1): 47-56.

[5] Wilkins Jr J E. Minimum Mass Thin Fins With Internal Heat Generation[J]. Nuclear Science and Engineering (US), 1962, 14.

[6] Liu C Y. A variational problem relating to cooling fins with heat generation[J]. Quarterly of Applied Mathematics, 1961, 19(3): 245-251.

[7] Natarajan U, Shenoy U V. Optimum shapes of convective pin fins with variable heat transfer coefficient[J]. Journal of the Franklin Institute, 1990, 327(6): 965-982.

[8] Hajabdollahi F, Rafsanjani H H, Hajabdollahi Z, et al. Multi-objective optimization of pin fin to determine the optimal fin geometry using genetic algorithm[J]. Applied Mathematical Modelling, 2012, 36(1): 244-254.

[9] Wang J, Wang X. The heat transfer optimization of conical fin by shape modification[J]. Chinese Journal of Chemical Engineering, 2016, 24(8): 972-978.

[10] Azarkish H, Sarvari S M H, Behzadmehr A. Optimum geometry design of a longitudinal fin with volumetric heat generation under the influences of natural

convection and radiation[J]. Energy Conversion and Management, 2010, 51(10): 1938-1946.

[11] Kern D Q, Kraus A D. Extended Surface Heat Transfer, McGraw-Hill, New York, 1972[J].

[12] Kundu B, Das P K. Optimum profile of thin fins with volumetric heat generation: a unified approach[J]. Journal of Heat Transfer, 2005, 127(8): 945-948.

[13] Azarkish H, Sarvari S M H, Behzadmehr A. Optimum design of a longitudinal fin array with convection and radiation heat transfer using a genetic algorithm[J]. International Journal of Thermal Sciences, 2010, 49(11): 2222-2229.

[14] Yeh R H. Errors in one-dimensional fin optimization problem for convective heat transfer[J]. International Journal of Heat and Mass Transfer, 1996, 39(14): 3075-3078.

[15] Fabbri G. A genetic algorithm for fin profile optimization[J]. International Journal of Heat and Mass Transfer, 1997, 40(9): 2165-2172.

[16] Fabbri G. Heat transfer optimization in internally finned tubes under laminar flow conditions[J]. International Journal of Heat and Mass Transfer, 1998, 41(10): 1243-1253.

[17] Fabbri G. Optimum profiles for asymmetrical longitudinal fins in cylindrical ducts[J]. International Journal of Heat and Mass Transfer, 1999, 42(3): 511-523.

[18] Fabbri G. Optimum performances of longitudinal convective fins with symmetrical and asymmetrical profiles[J]. International Journal of Heat and Fluid Flow, 1999, 20(6): 634-641.

[19] Copiello D, Fabbri G. Multi-objective genetic optimization of the heat transfer from longitudinal wavy fins[J]. International Journal of Heat and Mass Transfer, 2009, 52(5): 1167-1176.

[20] Bobaru F, Rachakonda S. Optimal shape profiles for cooling fins of high and low conductivity[J]. International Journal of Heat and Mass Transfer, 2004, 47(23): 4953-4966.

[21] Kang H S, Look Jr D C. Optimization of a thermally asymmetric convective and radiating annular fin[J]. Heat Transfer Engineering, 2007, 28(4): 310-320.

[22] Kang H S, Look Jr D C. Optimization of a trapezoidal profile annular fin[J]. Heat Transfer Engineering, 2009, 30(5): 359-367.

[23] Iqbal Z, Syed K S, Ishaq M. Fin design for conjugate heat transfer optimization in double pipe[J]. International Journal of Thermal Sciences, 2015, 94: 242-258.

[24] Kim D K. Thermal optimization of internally finned tube with variable fin thickness[J]. Applied Thermal Engineering, 2016, 102: 1250-1261.

[25] Nguyen Q, Yang C. Design of a longitudinal cooling fin with minimum volume by a modified Newton–Raphson method[J]. Applied Thermal Engineering, 2016, 98: 169-178.

[26] Bejan A. Constructal-theory network of conducting paths for cooling a heat generating volume[J]. International Journal of Heat and Mass Transfer, 1997, 40(4): 799813-811816.

[27] Wattez T, Lorente S. From pore network prediction based on the constructal law to macroscopic properties of porous media[J]. Journal of Physics D: Applied Physics, 2015, 48(48): 485503.

[28] González D, Amigo J, Lorente S, et al. Constructal design of salt-gradient solar pond fields[J]. International Journal of Energy Research, 2016, 40(10): 1428-1446.

[29] Ziaei S, Lorente S, Bejan A. Constructal design for convection melting of a phase change body[J]. International Journal of Heat and Mass Transfer, 2016, 99: 762-769.

[30] Bejan A, Lorente S. Design with constructal theory[M]. Hoboken: Wiley, 2008.

[31] Bejan A. Evolution as physics: The human & machine species[J]. European Review, 2017, 25(1): 140-149.

[32] Jany P, Bejan A. Ernst Schmidt's approach to fin optimization: an extension to fins with variable conductivity and the design of ducts for fluid flow[J]. International Journal of Heat and Mass Transfer, 1988, 31(8): 1635-1644.

[33] Bejan A, Errera M R. Technology evolution, from the constructal law: heat transfer designs[J]. International Journal of Energy Research, 2015, 39(7): 919-928.

[34] Bejan A. Heatlines (1983) versus synergy (1998)[J]. International Journal of Heat and Mass Transfer, 2015, 81: 654-658.

[35] Gosselin L, Bejan A, Lorente S. Combined ‘heat flow and strength’ optimization of geometry: mechanical structures most resistant to thermal attack[J]. International journal of heat and mass transfer, 2004, 47(14): 3477-3489.

[36] Bejan A, Lorente S, Lee J. Unifying constructal theory of tree roots, canopies and forests[J]. Journal of theoretical biology, 2008, 254(3): 529-540.

[37] Lorente S, Lee J, Bejan A. The “flow of stresses” concept: the analogy between mechanical strength and heat convection[J]. International Journal of Heat and Mass Transfer, 2010, 53(15): 2963-2968.

[38] Piegl L, Tiller W. The NURBS book[M]. Springer Science & Business Media, 2012.

[39] Versteeg H K, Malalasekera W. An introduction to computational fluid dynamics: the finite volume method[M]. Pearson Education, 2007.

[40] Deb K, Pratap A, Agarwal S, et al. A fast and elitist multiobjective genetic algorithm: NSGA-II[J]. IEEE Transactions on Evolutionary Computation, 2002, 6(2): 182-197.

[41] http://www.egr.msu.edu/~kdeb/codes.shtml (retrieved on 17/03/2017)